Structural and electronic properties of anisotropic ultrathin organic films from dichroic resonant soft x-ray reflectivity

Luca Pasquali,[1,2,3,*] Subhrangsu Mukherjee,[2,4,†] Fabio Terzi,[5] Angelo Giglia,[2] Nicola Mahne,[2,‡] Konstantin Koshmak,[1] Vladimir Esaulov,[6,7] Chiara Toccafondi,[8] Maurizio Canepa,[8] and Stefano Nannarone[1,2]

[1]*Dipartimento di Ingegneria 'Enzo Ferrari', Università di Modena e Reggio Emilia, Via Vignolese 905, 41125 Modena, Italy*

[2]*IOM-CNR, s.s. 14, Km. 163.5 in AREA Science Park, 34149 Basovizza, Trieste, Italy*

[3]*Department of Physics, University of Johannesburg, P.O. Box 524, Auckland Park, 2006, South Africa*

[4]*International Centre for Theoretical Physics, Strada Costiera 11, 34151 Trieste, Italy*

[5]*Dipartimento di Scienze Chimiche e Geologiche, Università di Modena e Reggio Emilia, Via Campi 183, 41125 Modena, Italy*

[6]*Université-Paris Sud, Institut des Sciences Moléculaires d'Orsay, Orsay, France*

[7]*CNRS, UMR 8214 Institut des Sciences Moléculaires d'Orsay, ISMO, Bâtiment 351, UPS-11, 91405 Orsay, France*

[8]*CNISM and Dipartimento di Fisica, Università di Genova, Via Dodecaneso 33, 16146 Genova, Italy*

(Received 15 April 2013; revised manuscript received 15 November 2013; published 2 January 2014)

We developed a quantitative approach for the determination of molecular arrangement and electronic structure in anisotropic organic ultrathin films based on the measurement of polarized reflectivity at the carbon K-edge. The reflectivity spectra were fitted to a parameterized model calculation. The method was applied to a self-assembled monolayer of 1,4-benzenedimethanethiol on gold. To simulate reflectivity, the organic anisotropic film was described by a dielectric tensor, obtained by *ab initio* calculations for the single molecule and suitable rotations to describe the molecular organization in film domains. Film structure was obtained though the best fit of the simulation to the experiment. Results were consistent with a monolayer-thick film composed of domains of molecules with in-plane isotropic distribution of orientations. In each domain, molecules adopted a standing configuration, with a tilt of 28° relative to the substrate normal. Information on the modification of the molecular electronic states due to chemical bonding was derived.

DOI: 10.1103/PhysRevB.89.045401 PACS number(s): 78.66.Qn, 68.55.−a, 78.20.Ci, 78.70.Ck

I. INTRODUCTION

The lineshape analysis of light scattering in photon-in–photon-out processes versus photon energy, photon polarization, incidence, and scattering geometry can disclose microscopic details of the surface and near-surface region of a system[1] through the spatial and energy dependency of the real and imaginary parts of the dielectric function.[2–6] In the near-visible range, optical constants of thin films and surfaces are commonly obtained thanks to consolidated specular reflectance techniques and related methodologies.[4,7–11] On the other hand, scattering techniques in the x-ray range, and especially specular reflectance at resonance, provide effective tools for refined atom and depth-resolved investigation of the chemical, structural, and magnetic[12–14] properties of a variety of systems, including organic materials.[15–22]

In this paper we considered the grazing incidence elastic-scattering process—polarized resonant soft x-ray reflectivity—at the carbon K-edge of an ultrathin organic film deposited on inorganic substrate. The measured reflectivity was simulated by a parameterized phenomenological model that was fitted to the experimental lineshape. The simulation was based on the propagation of the electromagnetic field in the vacuum/organic-film/substrate system, where the organic film was treated as an anisotropic material, described by a dielectric tensor. The elements of the tensor were derived calculating the anisotropic absorption cross section of the molecules through density functional theory (DFT) and subsequently applying the appropriate rotations to describe the arrangement of the molecules in the domains composing the film. The range of validity and applicability of a dielectric model in the description of ultrathin layers has been treated in references[7,9,10,23] for isotropic films. In this paper the range of application is extended to anisotropic films.

As a benchmark system we have chosen a 1,4-benzenedimethanethiol (BDMT) self-assembled monolayer (SAM) on polycrystalline Au(111). This choice was dictated by several reasons. Thiol and dithiol molecules containing aromatic rings are widely studied systems because of potential use in molecular electronics.[24–29] Moreover, in recent years we gained a detailed knowledge regarding the formation of BDMT SAMs on well-defined gold surfaces, exploiting both in-vacuum and in-liquid deposition, thanks to a systematic investigation by spectroscopic ellipsometry (SE), reflection-absorption infrared spectroscopy, electrochemistry measurements, photoemission, and x-ray absorption (XAS).[30–35] We elaborated a reliable protocol[30,35] for obtaining single-layer films with molecules in a standing up configuration, with a sulfur headgroup bonded to the substrate and the other S-H unbound group pointing upright. The films in the present study were prepared according to this protocol. While the film-building block (individual BDMT molecule) is relatively compact and simple to simulate with theoretical tools, the overall film structure is rather complex, due to the texturing of the substrate, the formation of domains with varying in-plane orientation, and the reciprocal molecular orientations within domains. This represents a typical realistic assembly situation, which can be encountered in many different fields, both basic and applicative, of organic thin films.

On one hand, our method provides a quantitative scheme to investigate ultrathin organic layers by polarized reflectivity at the C K-edge (an optical range of considerable general interest but requiring specific experimental care mainly in case of ultrathin films). On the other hand, it reduces the complex

situation of a multidomain organic anisotropic ultrathin film to a manageable problem, offering a clear and—though simple—physically rigorous framework to extract information on morphology, atomic geometry, and electronic properties of the film when these aspects simultaneously contribute to dichotic optical lineshape of the organic layer at the C K-edge.

The presented approach, based on calculated wavefunctions, constitutes an advancement with respect to similar works in literature,[15,16,22,36] where reflectivity is simulated using scalar–isotropic–dielectric constants derived from XAS experiments. The present method provides a direct insight into the involved atomic orbitals, and, in perspective, it paves the way toward a parameterized correction of the elements of the dielectric tensor to account for molecule-molecule and molecule-substrate interactions, which were neglected at this stage.

II. EXPERIMENTAL

Substrates were 200-nm-thick Au(111) polycrystalline films deposited on mica (from PHASIS). They were annealed at 600 °C for 30 s, followed by cooling under a N_2 flow. BDMT (98% purity, from Aldrich) was used without further purification. The SAMs were prepared by immersing the substrates into a N_2 degassed fresh 1-mM solution of n-hexane for about 30 min at 60 °C.[30] The samples were then rinsed with the same (fresh) solvent and dried with N_2. All these procedures were carried out in the absence of ambient light.

Specular reflectivity spectra were taken at the BEAR beamline[37,38] at the ELETTRA synchrotron (Trieste, Italy) using linearly polarized light (degree of linear polarization of 0.94) in the 280–320 eV range in *s*- and *p*-polarization incidence. The energy resolution and grazing incidence angle were 0.1 eV and 8.0°, respectively. Light intensity of direct and reflected beam was measured with a photodiode (IRD SXUV-100). The overall accuracy of reflectivity measurements was of the order of few units in 10^{-3}.

III. RESULTS AND DISCUSSION

Experimental reflectivity curves taken in *s*- and *p*-polarization incidence are shown in Figs. 1(a) and 1(b) as open dots. Electric fields within the media are indicated as E_{ij}, where i identifies the medium index and j the light polarization state ($j = 1, 3$ for inward s and p; $j = 2, 4$ for outward s and p).

The two *s*- and *p*-lineshapes present similar features, including the dominant structure in the 284–286 eV region and the additional modulations at higher energies. They also present individual peculiarities, which depend on the anisotropy of the film, clearly beyond the typical differences due to the different polarization incidences. The directional C1s $\rightarrow \pi^*$ excitation from the aromatic ring carbon atoms is responsible for the pronounced feature at about 285 eV, while C1s $\rightarrow \sigma^*$ excitations in the ring plane are predominantly responsible of the modulations at higher energy.[30,31,33]

In the simulation of light scattering by the vacuum/BDMT film/Au trilayer [insets of Figs. 1(a) and 1(b)], the Fourier-transformed wave equation $\vec{k}\vec{k} - |\vec{k}|^2 + (\omega/c)^2\overleftrightarrow{\varepsilon} = 0$ ($\vec{k}$ is the wave vector and the (complex) dielectric constant $\overleftrightarrow{\varepsilon}$ is a tensor for the film and a scalar for the substrate and vacuum) was solved in the whole space for *s*- (E_{01} field $\neq 0$, $E_{03} = 0$) and *p*- (E_{03} field $\neq 0$, $E_{01} = 0$) initial incident electric fields with the hypothesis that the fields (E_{22} and E_{24}) coming from $-\infty$ were zero. Elliptical polarization was generated in the propagating fields inside the anisotropic BDMT layer (E_{11}, E_{13}, E_{12}, and E_{14}) and in the reflected fields (E_{02}, E_{04}). The corresponding *s* and *p* reflectivity was calculated.

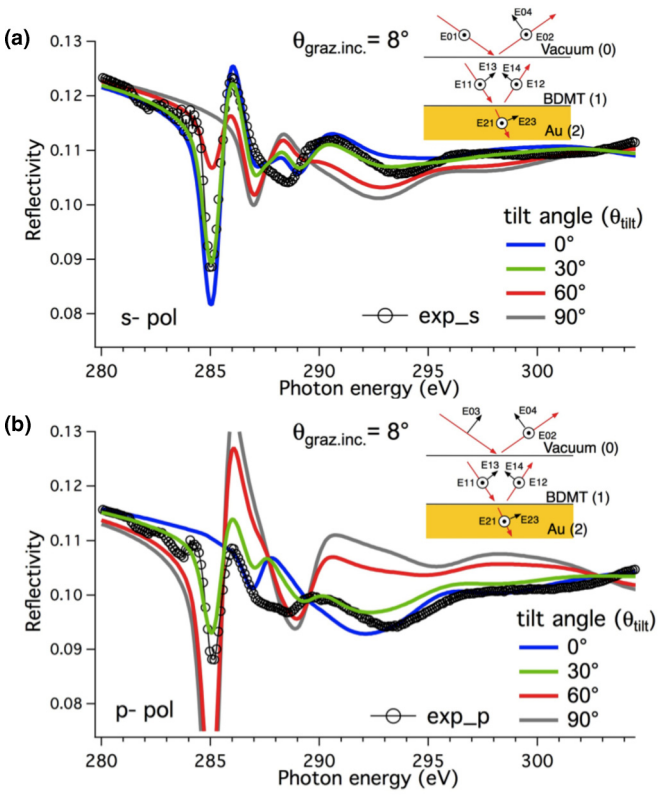

FIG. 1. (Color online) Reflectivity spectra taken in *s*- (a) and *p*- (b) geometries. The experimental spectra (exp_s and exp_p; open dots) are compared with simulations for a 1.5-nm-BDMT film on Au for different tilt angles of the molecules, following the model described in the text.

The mathematical scheme we followed[39] is of general validity. It can be applied to a layered medium composed of an unlimited number of anisotropic layers bonded to a semi-infinite vacuum and semi-infinite substrate. The calculation procedure follows that reported by Bertrand *et al.*[40] and extends to anisotropic media the method introduced in the pioneering works of Parratt[41] and Berreman.[42]

The model of the BDMT film used to simulate reflectivity was elaborated on the basis of the insights obtained in previous studies by photoemission, angular-dependent XAS, infrared spectroscopy, SE, and electrochemistry.[30–35] In these works, it was derived that the molecules adopted a standing configuration at the Au surface with the formation of S-Au bonding.

In this respect, it was assumed that the BDMT film had uniform thickness d and that it formed plane parallel abrupt interfaces [Fig. 2(a)]. It was further taken into account that the film had a multidomain structure with an in-plane random uniform distribution. This is physically due to the polycrystalline nature of the substrate, with the Au surface constituted by grains of prevailing (111) vertical orientation, and to the C_3 symmetry, or higher, of BDMT chemisorption on a generic (111) grain.

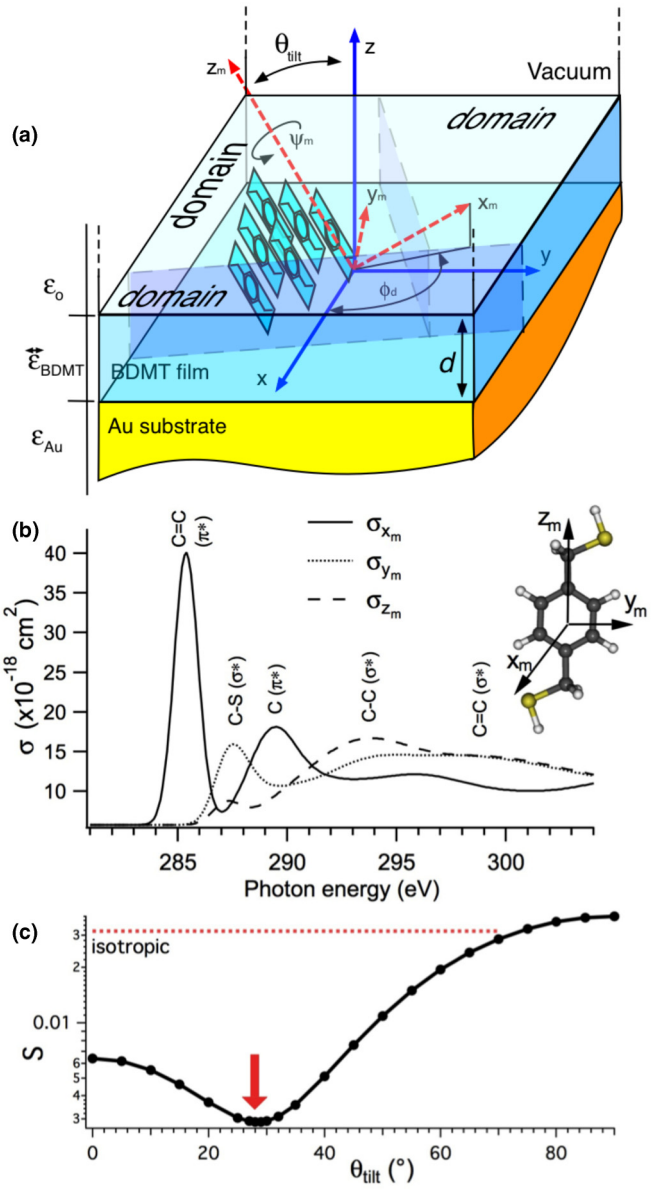

FIG. 2. (Color online) (a) Model of self-assembling. The molecular organization in a generic domain is shown (b). Calculated absorption cross sections σ_{x_m}, σ_{y_m}, and σ_{z_m} along the x_m, y_m, and z_m axes of the BDMT molecule. (c) Sum of the squared residuals S obtained from the comparison of the simulations for different tilt angles and fixed BDMT thickness $d = 1.5$ nm with the experiment, considering both s- and p-polarization spectra. An absolute minimum is found for $\theta_{\text{tilt}} = 28°$, as indicated by the arrow.

The molecular arrangement within a generic domain is shown in Fig. 2(a). In the adopted model, molecules in the domain were assumed parallel to each other, with the z_m long axes of the molecules forming an angle θ_{tilt} with the z axis of the substrate and the projections of the x_m axes on the substrate plane forming an angle ϕ_d with the x axis of the substrate. The y_m molecular axes were kept parallel to the xy plane of the substrate [the rotation angle ψ_m of the molecule around the long z_m axis was taken as zero in the calculation, as shown in Fig. 2(a)].

The substrate dielectric constant was taken from literature.[43] Concerning BDMT, in the generic domain shown in Fig. 2(a) with parallel aligned molecules, the principal optical axes coincide with the optical axes x_m, y_m, and z_m of the single molecule [Figs. 2(a) and 2(b)]. The dielectric tensor of the domain $\overleftrightarrow{\varepsilon}_M$ is diagonal in the x_m, y_m, and z_m frame, and along the principal axes the elements of the dielectric and refraction index tensors are related by the scalar expression $\tilde{\varepsilon}_{Mjj} = \tilde{n}^2_{Mjj}$ (with $j = x_m, y_m, z_m$). This allowed us to derive the elements of the tensor calculating the dichroic optical cross sections σ_j of the single molecules along x_m, y_m, and z_m and the bulk BDMT absorption coefficient $\alpha_j = N\sigma_j$, where N is the density of the molecules. Posing $\tilde{\varepsilon}_{Mjj} = \varepsilon'_{Mjj} + i\varepsilon''_{Mjj}$ and $\tilde{n}_{Mjj} = n'_{Mjj} + in''_{Mjj}$, recalling that $n'_{Mjj} = KK(n''_{Mjj})$ (KK indicates the Kramers-Kroenig transformation) and expressing $\alpha_j = 4\pi n''_{Mjj}/\lambda_0$, it can be seen that once σ_j is known, through Kramers-Kroenig transformations the complex values of the dielectric elements $\tilde{\varepsilon}_{Mjj}$ can be derived. The tensor $\overleftrightarrow{\varepsilon}_M$ obtained in this way is biaxial and diagonal in the x_m, y_m, and z_m frame, with $\tilde{\varepsilon}_{Mxx} \neq \tilde{\varepsilon}_{Myy} \neq \tilde{\varepsilon}_{Mzz}$.

The numerical values of the optical absorption cross sections σ_j of the single molecule [Fig. 2(b)] were calculated through DFT for the electric field polarized along x_m, y_m, and z_m. In first approximation, the interactions of the molecules between themselves and with the substrate were not taken into account. The calculation was carried out using the Slater transition state method[44,45] through the code StoBe.[46] The geometry of the free molecule was first optimized, following the scheme outlined in Ref. 31. Dipole transitions and angle-dependent absorption at the K-edge were calculated at all nonequivalent C atomic centers. An IGLO-III basis on each excitation center was used to better describe relaxation effects. Effective core potentials were used for the remaining carbon atoms. The dipole-excitation spectra obtained in this way were Gaussian convoluted with an energy-dependent broadening. For a correct energy scale alignment of the absorption spectra of nonequivalent centers, an additional ΔKohn−Sham adjustment[47,48] was applied to the lowest core-excited state for each center.

The three calculated cross sections were normalized by rescaling them, well below the C K-edge, to the absorption coefficient of an isotropic medium with a partial concentration of chemical species according to the molecular stoichiometry (C_8H_9S) and obtained from atomic tabulated values.[43] The first pronounced peak at about 285 eV of photon energy is associated with the excitation into the π^* states of the aromatic ring; the second structure is related to a transition to C–S/σ^* orbital, involving the C atoms in the methylene groups; the third feature is similarly associated to a transition to π^* states of the aromatic ring; the fourth and fifth broad structures are assigned to transitions to σ^* levels.[31] The π^* and σ^* transitions are observed when the electric field of the incoming light is oriented along the x_m molecular axis, perpendicular to the aromatic ring plane, and when the electric field vector is in the $y_m z_m$ molecular plane, respectively.

The density of the molecules, $N = 4.0 \times 10^{21}$ cm^{-3}, was taken constant in all domains, and it was fixed by assuming that the mass density of the film corresponded to that of the bulk material, $\rho = 1.134$ g/cm^3. This is compatible with

experimental results of standing thiol molecules on Au(111).[31] Other realistic values of N in the range 3–5 $\times$ 10^{21} cm^{-3} were also tested, leading to comparable results (not shown here).

In the simulation, the propagation of the fields had to be calculated in the xyz frame of the substrate. To this end, the $\overleftrightarrow{\varepsilon}_M$ tensor was rotated by the tilt angle θ_{tilt} and the azimuthal angle ϕ_d, in consistence with the rotation of the domain with respect to the substrate axes [Fig. 2(a)]. By applying rotation matrices $R(\theta_{\text{tilt}}, \varphi_d)$ to $\overleftrightarrow{\varepsilon}_M$, a new tensor $\overleftrightarrow{\varepsilon}_d$ describing the generic domain in the xyz frame was then obtained, according to the relation $\overleftrightarrow{\varepsilon}_d(\theta_{\text{tilt}}, \varphi_d) = R^T(\theta_{\text{tilt}}, \varphi_d)\overleftrightarrow{\varepsilon}_M R(\theta_{\text{tilt}}, \varphi_d)$, where R^T is the transposed matrix.

The dielectric tensor of whole BDMT film was finally constructed applying a space average over multiple domains, all of them sharing the same θ_{tilt} angle. We operated an average over the azimuthal angle ϕ_d, giving rise to in-plane isotropy. This average was performed under the assumptions that the beam footprint was large enough ($\sim$100 μm^2) to subtend a large number of domains, that the scattered intensity from different domains added up incoherently to contribute to the total reflected signal and that the domains had random distributions of in-plane orientations. On the basis of beam/field parameters (wavelength, energy resolution, and beam divergence $<$ 20 mrad) and the expected domain dimensions (of the order of 10–20 nm or below), diffraction/interference effects from domain structures and from their crystalline structure were neglected. These assumptions appear of wide validity for organic thin films on polycrystalline substrates.

The average dielectric tensor of the whole BDMT layer is given by

$$\overleftrightarrow{\tilde{\varepsilon}}(\theta_{\text{tilt}}) = \frac{1}{(2\pi)}\int_0^{2\pi} \overleftrightarrow{\tilde{\varepsilon}}_d(\theta_{\text{tilt}},\varphi_d)\,d\varphi_d$$

$$= \begin{pmatrix} \frac{1}{2}(\tilde{\varepsilon}_{Mxx}\cos^2\theta_{\text{tilt}} + \tilde{\varepsilon}_{Mzz}\sin^2\theta_{\text{tilt}}) + \frac{1}{2}\tilde{\varepsilon}_{Myy} & 0 & 0 \\ 0 & \frac{1}{2}(\tilde{\varepsilon}_{Mxx}\cos^2\theta_{\text{tilt}} + \tilde{\varepsilon}_{Mzz}\sin^2\theta_{\text{tilt}}) + \frac{1}{2}\tilde{\varepsilon}_{Myy} & 0 \\ 0 & 0 & (\tilde{\varepsilon}_{Mxx}\cos^2\theta_{\text{tilt}} + \tilde{\varepsilon}_{Mzz}\sin^2\theta_{\text{tilt}}) \end{pmatrix}.$$

It is diagonal and uniaxial, depending on the single parameter θ_{tilt}. Within this model, films thicker than one monolayer, which is not the present case, can be thought of as a stack of single-layer-thick molecular films, in principle each of them with its own geometry and specific dielectric tensor.

It resulted that θ_{tilt} and the layer thickness d were the only free parameters to fit the model lineshape to the experiment. In Figs. 1(a) and 1(b), the simulated reflectivities calculated at different θ_{tilt} angles (here shown only for 0°, 30°, 60°, and 90°) are compared to the experimental curves in s- and p-polarization incidence for d = 1.5 nm. A marked dependence of the lineshape on θ_{tilt} was obtained, demonstrating the sensitivity of our approach to the geometry of self-assembling. This was possible also because the electronic properties of BDMT and the related anisotropies are robust toward molecular-molecular and molecular-substrate interactions, and in the film they preserve the overall isolated molecule characteristics. The best fit was obtained calculating the sum S of the squared residuals from the comparison of both the s- and p-experimental curves with the simulations, as a function of θ_{tilt}, as shown in Fig. 2(c) (in steps of 5° or 1° close to minimum). A minimum was found for $\theta_{\text{tilt}} = 28° \pm 2°$. This result is to be related with previous findings in Refs. 30 and 33, where analogous values of tilt angles were inferred by angular dependent XAS in total electron yield. For comparison purposes, the S value relative to a random (isotropic) molecular distribution is also shown as a horizontal broken line. This clearly demonstrates the anisotropic optical properties of the film.

To test the sensitivity of the procedure, a different molecular arrangement within domains was also simulated, with the molecules adopting a herringbone structure, as suggested for benzenethiol.[49] The result is shown in Fig. 3, where simulations for a herringbone arrangement are compared with the parallel alignment presented above. Simulations refer to a tilt angle of 28°. For simplicity, the dielectric tensor of the herringbone configuration was constructed supposing that adjacent molecules in each domain were alternately rotated by $\psi_m = 0$ and $-90°$ in a mutually perpendicular arrangement, as shown in the insets of Fig. 3. In this case, $\overleftrightarrow{\varepsilon}_M$ was obtained through an average with equal weights of the two different molecular orientations, with $\psi_m = 0$ and $-90°$.

In s-polarization [Fig. 3(a)], the two configurations do not differ significantly, except for a slight amplification of the π^* resonance at 285 eV for the herringbone arrangement. Major differences occur in p-polarization [Fig. 3(b)]. In particular, the first structure associated to the π^* resonance at 285 eV is pronouncedly reduced for the herringbone arrangement, failing to reproduce the experiment. In this configuration, in fact, 50% of the benzene ring planes are perpendicularly oriented with respect to the surface plane, independently of the tilt angle, and they do not contribute to the p-reflectivity signal. Consequently, the overall agreement of simulation with the experiment for both s- and p-polarizations was inferior with respect to the parallel alignment of molecules discussed above. The goal of this comparison, forcedly not exhaustive, is not to exclude the possibility of other molecular arrangements, better fitting the model to experiment. Instead, it evidences the sensitivity of the method to the details of the interplay between the geometrical and electronic structures of the film.

Besides the tilt angle, the monolayer thickness d is another free parameter. It represents the distance between regions where the soft x-ray photon propagating in the film feels the change of electronic properties at the vacuum-film and film-substrates interfaces. Several values of d were tested in the range 0.5–3 nm. The effect of film thickness is shown in Fig. 4. Simulations prove the sensitivity of the method to

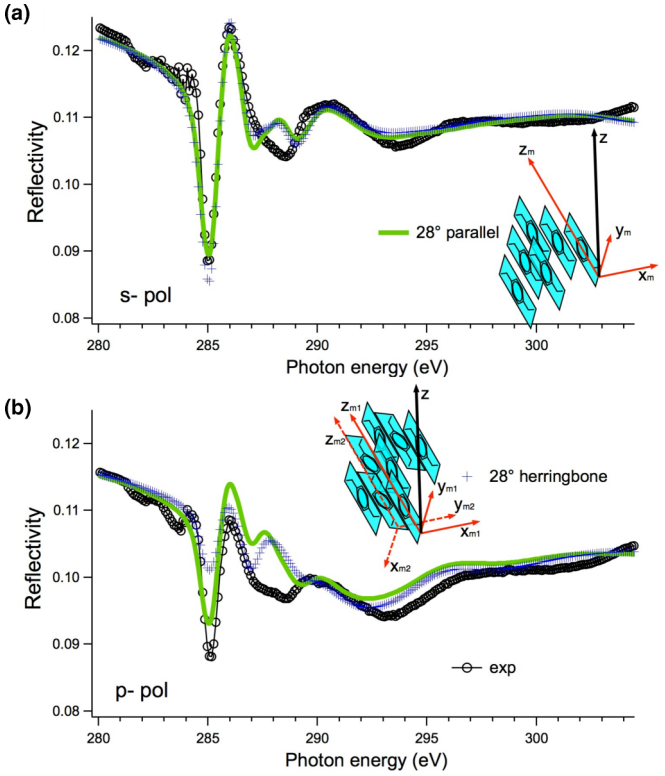

FIG. 3. (Color online) Comparison between different molecular configurations (parallel and herringbone) in each domain for (a) s- and (b) p-polarization. Simulations refer to $\theta_{\text{tilt}} = 28°$ and $d = 1.5$ nm. In the herringbone configuration, the relative orientations of the two molecular frames composing the domain and corresponding to $\psi_m = 0°$ (x_{m1}, y_{m1}, z_{m1}) and $-90°$ (x_{m2}, y_{m2}, z_{m2}) are reported.

small variations of layer thickness. While reflectivity in the pre-edge region is substantially determined by the substrate, changes of film thickness in the subnanometer range (with same molecular density) show pronounced variations in the edge region between 285 eV and 300 eV. Best agreement with the experiment was found through fitting, following an approach analogous to the one used for the determination of the molecular tilt angle. The sum S of the squared residuals from the comparison of both the s- and p-experimental curves with the simulations is shown in Fig. 2(c) as a function of the film thickness. A minimum was found for a thickness $d =$ 1.5 nm, which is compatible with independent evaluations derived from SE in the visible light spectral range.[35] This value was used in all other simulations presented in this paper.

Together with atomic geometry and morphological parameters, the method provided the elements of dielectric tensor of the anisotropic BDMT monolayer. The three elements are shown in Fig. 5 and correspond to the structure of Fig. 2(a).

We stress that these elements do not contain molecular-molecular and molecular-substrate contributions. In this respect, the misfit between experiment and simulation, especially in the 287–289 eV region is physically meaningful. It indicates how the chemisorption process affects the electronic properties of BDMT, in particular its influence on the C-S bonding (at 287 eV) at the bonding side and on the π^*-σ^* states, due to molecule-molecule interactions and some degree of

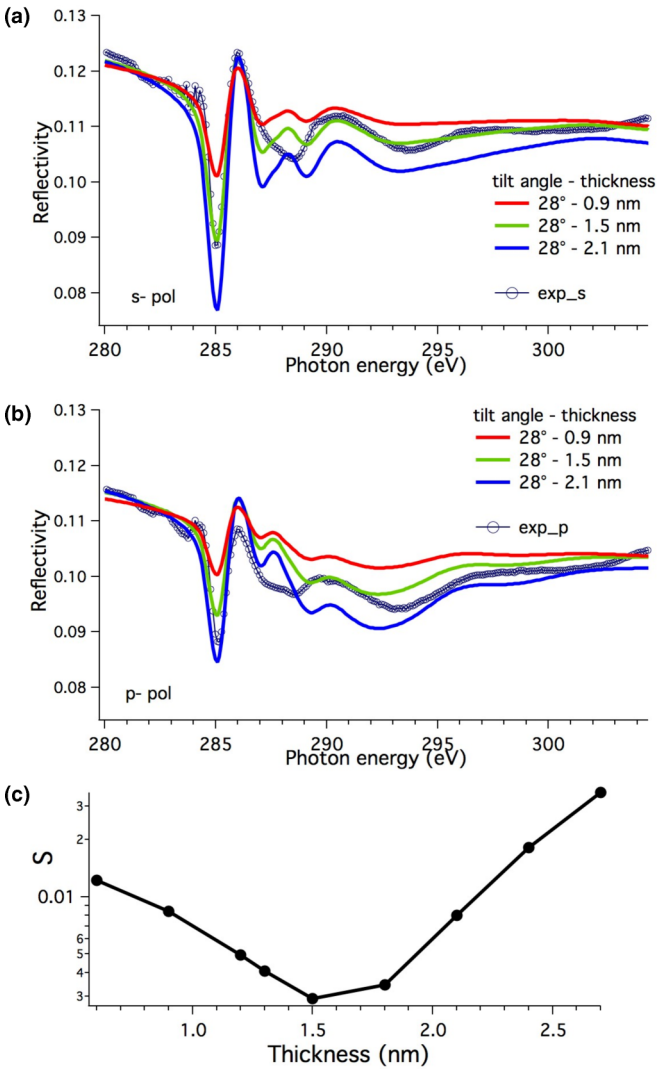

FIG. 4. (Color online) Effect of film thickness in (a) s- and (b) p-polarization. Simulations refer to $\theta_{\text{tilt}} = 28°$ for the molecular parallel alignment, proposed in Fig. 2(a). (c) Sum of the squared residuals for both s- and p-polarization from the comparison of the simulations for different thickness with the experiment.

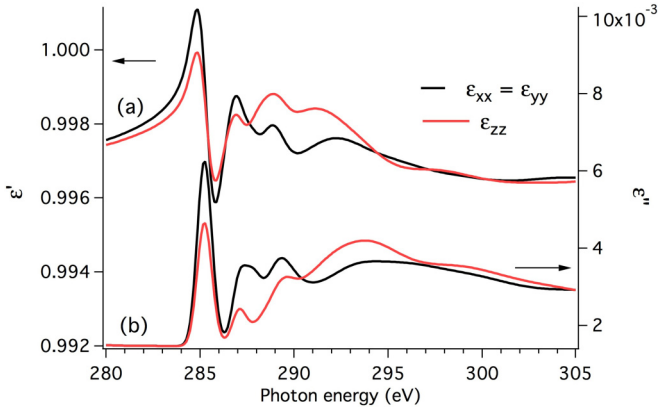

FIG. 5. (Color online) (a) Real and (b) imaginary parts of the elements of the BDMT tensor $\vec{\vec{\varepsilon}}$ ($\theta_{\text{tilt}} = 28°$), $d = 1.5$ nm, molecular parallel arrangement of Fig. 2(a).

hybridization with substrate states and possibly to peculiar steric conformation of the molecules that were not considered here. In perspective, the matrix elements of the different optical transitions of Fig. 2(b) can be parameterized to improve the fitting to the experiment and to single out the spectral regions where the optical properties deviate from that of noninteracting molecules. However, it is noteworthy that in spite of the simplifications of the model and of the lack of adjustable parameters, most of the experimental features were reproduced by the simulation, even in absolute magnitude. Interface roughness was also not taken into account in the model. Nevertheless, it may be expected that in this case interface roughness can affect the overall intensity but not the overall lineshape and relative intensities.

IV. CONCLUSIONS

In summary, we have demonstrated that rich quantitative information regarding structure, morphology, and electronic-chemical properties of an anisotropic organic monolayer film can be obtained through a detailed study of the lineshape of specular polarized reflectivity at the carbon K-edge. This is based on fitting the experimental reflectivity with a simulation through the calculation of the propagation of the electromagnetic field in the vacuum/organic film/substrate system. The organic film was treated as an anisotropic medium, described by a dielectric tensor. We applied the method to a single layer of 1,4-BDMT on polycrystalline gold. Best fitting of the simulations to the experiment indicated that the film had a multidomain structure, with the molecules adopting a standing, parallel-aligned packing in each domain, with an average tilt angle of 28° with respect to the substrate normal. A thickness of 1.5 nm was obtained for the film. Its anisotropic dielectric constants were derived from *ab initio* DFT calculations of the anisotropic absorption cross section of the single molecules. The application of this method to different edges is straightforward.

We believe that the approach followed in this paper will open interesting applications to a variety of organic thin films, especially when other experimental techniques cannot be straightforwardly applied. It provides a scheme for quantitative investigation, for instance in those cases where electron spectroscopy cannot be employed because of the presence of nonconductive materials, of applied electrical or magnetic fields, or the regions of interest are buried at distances from the surface higher than electron-probe sampling depth. The method described here can be easily extended to multilayer anisotropic films also in the presence of different self-assembling in each layer.

ACKNOWLEDGMENTS

We acknowledge financial assistance from the France-Italy CNRS PICS agreement, Sincrotrone Trieste, and from the FP7-IRSES-2009 Project No. 247518 (ONDA). The experiments were carried out with Proposals No. 20095205, No. 20110184, and No. 20115276 at ELETTRA. A. De Luisa, R. Fanucchi, F. Salvador, and P. Bertoch are acknowledged for their precious support. One of us (SN) is indebted to A. Verna for stimulating discussions. SM is indebted with Prof. H. Ade for precious and fruitful discussions.

*Corresponding author: luca.pasquali@unimore.it
†Present address: Department of Physics, North Carolina State University, Raleigh, NC 27695-8202, USA.
‡Present address: Sincrotrone Trieste s.s. 14 - km 163,5 in AREA Science Park, 34149 Basovizza, Trieste Italy.

[1] M. Born and E. Wolf, *Principles of Optics*, 7th Ed. (University Press, Cambridge, 1999).
[2] J. Als-Nielsen, *Elements of Modern X-Ray Physics* (Wiley, New York, 2001).
[3] J. Daillant and A. Gibaud, *X-Ray and Neutron Reflectivity: Principles and Applications* (Springer, Berlin Heidelberg, 2009).
[4] H. Fujiwara, *Spectroscopic Ellipsometry: Principles and Applications* (John Wiley & Sons Ltd., Chichester, England, 2007).
[5] M. Tolan, *X-Ray Scattering from Soft-Matter Thin Films* (Springer, Berlin Heidelberg, 1999).
[6] H. G. Tompkins and W. A. McGahan, *Spectroscopic Ellipsometry and Reflectometry: A Users Guide* (John Wiley and Sons, New York, 1999).
[7] R. Del Sole, in *Photonic Probes of Surfaces*, edited by P. Halevi (Elsevier, Amsterdam, 1995), p. 131.
[8] M. Dressel, B. Gompf, D. Faltermeier, A. K. Tripathi, J. Pflaum, and M. Schubert, Opt. Express **16**, 19770 (2008).
[9] J. D. Mcintyre and D. E. Aspnes, Surf. Sci. **24**, 417 (1971).
[10] P. Weightman, D. S. Martin, R. J. Cole, and T. Farrell, Rep. Prog. Phys. **68**, 1251 (2005).
[11] M. Prato, R. Moroni, F. Bisio, R. Rolandi, L. Mattera, O. Cavalleri, and M. Canepa, J. Phys. Chem. C **112**, 3899 (2008).
[12] M. Sacchi and A. Mirone, Phys. Rev. B **57**, 8408 (1998).
[13] K. H. Stone, S. M. Valvidares, and J. B. Kortright, Phys. Rev. B **86**, 024102 (2012).
[14] A. Verna, B. A. Davidson, Y. Szeto, A. Y. Petrov, A. Mirone, A. Giglia, N. Mahne, and S. Nannarone, J. Magn. Magn. Mater. **322**, 1212 (2010).
[15] H. Ade, C. Wang, A. Garcia, H. Yan, K. E. Sohn, A. Hexemer, G. C. Bazan, T. Q. Nguyen, and E. J. Kramer, J. Polym. Sci. Pol. Phys. **47**, 1291 (2009).
[16] B. A. Collins, J. E. Cochran, H. Yan, E. Gann, C. Hub, R. Fink, C. Wang, T. Schuettfort, and C. R. McNeill, M. L. Chabinyc, and H. Ade, Nat. Mater. **11**, 536 (2012).
[17] C. R. McNeill, B. Watts, L. Thomsen, W. J. Belcher, N. C. Greenham, P. C. Dastoor, and H. Ade, Macromolecules **42**, 3347 (2009).
[18] M. Mezger, B. Jerome, J. B. Kortright, M. Valvidares, E. M. Gullikson, A. Giglia, N. Mahne, and S. Nannarone, Phys Rev B **83**, 155406 (2011).
[19] C. Wang, T. Araki, and H. Ade, Appl. Phys. Lett. **87**, 214109 (2005).

[20]C. Wang, T. Araki, B. Watts, S. Harton, T. Koga, S. Basu, and H. Ade, J. Vac. Sci. Technol. A **25**, 575 (2007).
[21]C. Wang, A. Garcia, H. P. Yan, K. E. Sohn, A. Hexemer, T. Q. Nguyen, G. C. Bazan, E. J. Kramer, and H. Ade, J. Am. Chem. Soc. **131**, 12538 (2009).
[22]H. Yan, C. Wang, A. R. McCarn, and H. Ade, Phys. Rev. Lett **110**, 177401 (2013).
[23]S. Nannarone and S. Selci, Phys. Rev. B **28**, 5930 (1983).
[24]R. P. Andres, T. Bein, M. Dorogi, S. Feng, J. I. Henderson, C. P. Kubiak, W. Mahoney, R. G. Osifchin, and R. Reifenberger, Science **272**, 1323 (1996).
[25]W. Azzam, P. Cyganik, G. Witte, M. Buck, and C. Woll, Langmuir **19**, 8262 (2003).
[26]H. T. Rong, S. Frey, Y. J. Yang, M. Zharnikov, M. Buck, M. Wuhn, C. Woll, and G. Helmchen, Langmuir **17**, 1582 (2001).
[27]A. Shaporenko, M. Brunnbauer, A. Terfort, M. Grunze, and M. Zharnikov, J. Phys. Chem. B **108**, 14462 (2004).
[28]Y. Tai, A. Shaporenko, H. T. Rong, M. Buck, W. Eck, M. Grunze, and M. Zharnikov, J. Phys. Chem. B **108**, 16806 (2004).
[29]M. Zharnikov, S. Frey, H. Rong, Y. J. Yang, K. Heister, M. Buck, and M. Grunze, Phys. Chem. Chem. Phys. **2**, 3359 (2000).
[30]L. Pasquali, F. Terzi, R. Seeber, S. Nannarone, D. Datta, C. Dablemont, H. Hamoudi, M. Canepa, and V. A. Esaulov, Langmuir **27**, 4713 (2011).
[31]L. Pasquali, F. Terzi, R. Seeber, B. P. Doyle, and S. Nannarone, J. Chem. Phys. **128**, 134711 (2008).
[32]L. Pasquali, F. Terzi, C. Zanardi, R. Seeber, G. Paolicelli, N. Mahne, and S. Nannarone, J. Phys.: Condens. Matter **19**, 305020 (2007).
[33]L. Pasquali, F. Terzi, C. Zanardi, L. Pigani, R. Seeber, G. Paolicelli, S. M. Suturin, N. Mahne, and S. Nannarone, Surf Sci **601**, 1419 (2007).
[34]L. S. Alarcon, L. Chen, V. A. Esaulov, J. E. Gayone, E. A. Sanchez, and O. Grizzi, J. Phys. Chem. C **114**, 19993 (2010).
[35]H. Hamoudi, M. Prato, C. Dablemont, O. Cavalleri, M. Canepa, and V. A. Esaulov, Langmuir **26**, 7242 (2010).
[36]C. R. McNeill and H. Ade, J. Mater. Chem. C **1**, 187 (2013).
[37]L. Pasquali, A. DeLuisa, and S. Nannarone, AIP Conf. Proc. **705**, 1142 (2004).
[38]S. Nannarone, F. Borgatti, A. DeLuisa, B. P. Doyle, G. C. Gazzadi, A. Giglia, P. Finetti, N. Mahne, L. Pasquali, M. Pedio, G. Selvaggi, G. Naletto, M. G. Pelizzo, and G. Tondello, AIP Conf. Proc. **705**, 450 (2004).
[39]N. Mahne, A. Giglia, L. Sponza, A. Verna, and S. Nannarone, in *Seventh International Conference on Thin Film Physics and Applications*, *79951S* (Proc. SPIE 7995, 2011).
[40]P. Bertrand, C. Hermann, G. Lampel, J. Peretti, and V. I. Safarov, Phys. Rev. B **64**, 235421 (2001).
[41]L. G. Parratt, Phys. Rev. **95**, 359 (1954).
[42]D. W. Berreman, J. Opt. Soc. Am. **62**, 502 (1972).
[43]B. L. Henke, E. M. Gullikson, and J. C. Davis, At. Data Nucl. Data Tables **54**, 181 (1993).
[44]J. C. Slater, edited by P. O. Loewdin (Academic Press, 1972), p. 1.
[45]J. C. Slater and K. H. Johnson, Phys. Rev. B **5**, 844 (1972).
[46]K. Hermann, L. G. M. Pettersson, M. E. Casida, C. Daul, A. Goursot, A. Koester, E. Proynov, A. St-Amant, D. R. Salahub, V. Carravetta, H. Duarte, C. Friedrich, N. Godbout, J. Guan, C. Jamorski, M. Leboeuf, M. Leetmaa, M. Nyberg, S. Patchkovskii, L. Pedocchi, F. Sim, L. Triguero, and A. Vela, StoBe-deMon version 3.1, 2011.
[47]M. Cavalleri, M. Odelius, D. Nordlund, A. Nilsson, and L. G. M. Pettersson, Phys. Chem. Chem. Phys. **7**, 2854 (2005).
[48]C. Kolczewski, R. Puttner, O. Plashkevych, H. Agren, V. Staemmler, M. Martins, G. Snell, A. S. Schlachter, M. Sant'Anna, G. Kaindl, and L. G. M. Pettersson, J. Chem. Phys. **115**, 6426 (2001).
[49]J. Nara, S. Higai, Y. Morikawa, and T. Ohno, J. Chem. Phys. **120**, 6705 (2004).